AKADÉMIAI KIADÓ

Dam-break computations by a finite volume on dry regions

Farid Boushaba[1], Salah Daoudi[2], Ahmed Yachouti[2] and Youssef Regad[3]*

[1] Faculty of Science, National School of Applied Sciences, BP 669, Oujda, Morocco

[2] Sciences Faculty, 1st Mohamed University, Oujda, Morocco

[3] Industrial and Seismic Engineering Team, National School of Applied Sciences, BP 669, Oujda, Morocco

Pollack Periodica • An International Journal for Engineering and Information Sciences

17 (2022) 1, 117–122

DOI:
10.1556/606.2021.00428

Received: April 5, 2021 • Revised manuscript received: June 17, 2021 • Accepted: June 19, 2021
Published online: November 16, 2021

ORIGINAL RESEARCH PAPER

ABSTRACT

This paper presents numerical solvers, based on the finite volume method. This scheme solves dam break problems on the dry bottom in 2D configuration. The difficulty of the simulation of this type of problem lies in the propagation of shocks on the dry bottom. The equation model used is the shallow water equations written in conservative form. The scheme used is second order in space and time. The method is modified to treat dry bottoms. The validity of the method is demonstrated over the dam break example. A comparison with finite elements shows the weakness and robustness of each method.

KEYWORDS

shock capturing, Roe's solver, finite volume method, MinMod limiter, balanced scheme

1. INTRODUCTION

Among natural disasters, floods are the most destructive in terms of magnitude and human impact. Floods often cause considerable damage to properties, demanding huge financial sums for repair works, the temporary closure of businesses and the uprooting of families from homes. For example Morocco recorded no less than 35 episodes of floods between 1951 and 2015. there are 391 sites are subject to flood risks in Morocco [1, 2]. For these reasons, the development of digital resolution models is very necessary, in order to predict floods and provide for hydraulic structures to reduce material and human damage.

The class of the shallow-water equations, modeling by the equations of Saint-Venant, it is a very studied subject in hydraulic construction and in applied mathematics. Indeed, the dam break problem was simulated and compared on dry bed with a second order centered scheme written in finite element method [3–5] and the determination of the water depth and the velocities field contributes to the design of the hydraulic structures like bridges, water transport, dams and the planning of resources in water is also of a fundamental importance, notably the prediction of the ruptures of the dams [6, 7]. Several numeric method classes are used in the literature to solve the equations of Saint-Venant, each having its merits and its weak points. This work uses modified Roe scheme for dry beds treatment in finite volume version. The finite volume method also solves numerically the shallow water equations. Many schemes and algorithm has received considerable attention in the past two decades, like for instance [8–11]. This work presents a finite volume scheme of Roe based on the Riemann solver [12]. To increase accuracy, the paper uses second order accuracy by using Monotonic Upstream-centered Scheme for Conservation Laws (MUSCL) technique incorporating limiters. Since the original version of this solver cannot handle problems with dry beds, and it does not guarantee the entropicity of the scheme, the work presents the modifications, which

*Corresponding author.
E-mail: y.regad@ump.ac.ma

AKJournals

has made to correct the scheme without the use of a threshold parameter. The Total Variation Diminishing (TVD) Runge-Kutta scheme was used by [13] to solve the wet bed sluice gate dam-break and circular dam-break problems.

2. MATHEMATICAL MODEL

The free surface flow in a domain Ω of border Γ is governed by Saint-Venant equations, and they are presented in 2D case under de following form:

$$\frac{\partial \mathbf{U}}{\partial t}+\frac{\partial \mathbf{F}}{\partial x}+\frac{\partial \mathbf{G}}{\partial y}=\mathbf{S} \tag{1}$$

with

$$\mathbf{U}=\begin{Bmatrix} h \\ hu \\ hv \end{Bmatrix}, \quad \mathbf{F}=\begin{Bmatrix} hu \\ hu^2+0.5h^2 \\ huv \end{Bmatrix}, \quad \mathbf{G}=\begin{Bmatrix} hv \\ huv \\ hv^2+0.5gh^2 \end{Bmatrix}, \quad \mathbf{S}=\begin{Bmatrix} 0 \\ -ghS_{fx} \\ -ghS_{fy} \end{Bmatrix} \tag{2}$$

u and v are the velocity components in the x and y directions and h is the water height. S_{fx} and S_{fy} are the bed friction terms in the x and y directions.

3. FINITE VOLUME ROE SCHEME

3.1. Discretization

This part presents only mean stages of the scheme. The integration of Eq. (1) is (without source term) evaluated over a finite volume T_i, the application of Green formula leads to:

$$A(t_i)\frac{\partial \mathbf{U}}{\partial t}+\sum_{j\in E(i)}\int_{\Gamma_{ij}}\left(\mathbf{F}n_x+\mathbf{G}n_y\right)d\Gamma=0 \tag{3}$$

where $A\ (t_i)$ is the area of triangular cell T_i; Γ_{ij} denotes the interface between cells T_i and T_j; $E(i)$ is the set of triangles that have a common edge with triangle T_i, $\boldsymbol{n}_{ij}(n_x;\ n_y)$ is the outward unit normal to the boundary of cell T_i to T_j. The «cell-centered» finite volumes formulation was considered, which supposes that the control volumes coincide with the mesh triangles and that the unknown are the average states on each of these control volumes. The problem is to evaluate the convection flux $\mathscr{F}(\mathbf{U},\ \mathbf{n})=\mathbf{F}n_x+\mathbf{G}n_y$ over the three borders of the cell T_i. The approximate Riemann solver developed by [12] is based on characteristic decomposition of the flux differences while insuring the conservation properties of the scheme:

$$\begin{aligned}\Phi\left(U_i,\ U_j,\ n_{ij}\right)&=\frac{1}{2}\left(\mathscr{F}\left(U_i,\ n_{ij}\right)+\mathscr{F}\left(U_j,\ n_{ij}\right)\right)-\\ &-\frac{1}{2}\left|\tilde{\mathscr{A}}\left(U_i,\ U_j,\ n_{ij}\right)\right|\left(U_j-U_i\right)\end{aligned} \tag{4}$$

where $\tilde{\mathscr{A}}$ [14] is a constant matrix at every time level and for each pair of states U_i and U_j. $\tilde{\mathscr{A}}$ must verify the following conditions:

– Conservation of the scheme;
– The consistency with the original problem;
– Property of hyperbolicity.

With the parameter vector, the formula becomes:

$$\tilde{\mathbf{U}}\left(U_i,\ U_j\right)=\begin{cases}\tilde{h}=\dfrac{1}{2}\left(h^i+h^j\right)\\ \tilde{u}=\dfrac{u^i\sqrt{h^i}+u^j\sqrt{h^j}}{\sqrt{h^i}+\sqrt{h^j}},\\ \tilde{v}=\dfrac{v^i\sqrt{h^i}+v^j\sqrt{h^j}}{\sqrt{h^i}+\sqrt{h^j}}\end{cases} \tag{5}$$

where

$$\mathscr{A}(\mathbf{U},\ \boldsymbol{n})=n_x\frac{\partial \mathbf{F}}{\partial U}+n_y\frac{\partial \mathbf{G}}{\partial U}=$$
$$=\begin{bmatrix}0 & n_x & n_y\\ \left(gh-u^2\right)n_x-uvn_y & 2un_x-vn_y & un_y\\ \left(gh-v^2\right)n_y-uvn_x & vn_x & un_x+2vn_y\end{bmatrix}. \tag{6}$$

With the next decomposition of the Jacobian matrix:

$$|\mathscr{A}|=\mathscr{A}^+-\mathscr{A}^- \tag{7}$$

Then $\tilde{\mathscr{A}}$ is defined as:

$$\tilde{\mathscr{A}}\left(U_i,U_j,\boldsymbol{n}_{ij}\right)=\mathscr{A}\left(\tilde{\mathbf{U}}\left(U_i,\ U_j\right),\ \mathbf{n_{ij}}\right) \tag{8}$$

where $\mathscr{A}$ contains all $\mathscr{A}^+$ positive and $\mathscr{A}^-$ negative eigenvalues, the Rankine-Hugoniot condition allows a simplification of the numerical flux form in Eq. (9), which can be written in the following ways:

$$\Phi\left(U_i,\ U_j,\ n_{ij}\right)=\mathscr{F}\left(U_j,\ n_{ij}\right)-\mathscr{A}^+\left(\tilde{\mathbf{U}},\ n_{ij}\right)\left(U_j-U_i\right) \tag{9}$$

and

$$\Phi\left(U_i,\ U_j,\ n_{ij}\right)=\mathscr{F}\left(U_j,\ n_{ij}\right)-\mathscr{A}^-\left(\tilde{\mathbf{U}},\ n_{ij}\right)\left(U_j-U_i\right) \tag{10}$$

The great advantage of these formulations, especially in the context of the study of transport of multiple contaminants in shallow water flows, is the low computational effort. There as on for this fact is that at most one eigenvalue of the system has a different sign from all others. Then one of the two terms $\mathscr{A}^+$ or $\mathscr{A}^-$ contains at most one eigenvalue, thus becoming very simple to evaluate [14].

3.2. Roe scheme second order

The Roe scheme is upwind first order accuracy scheme, to increase the order of accuracy the MUSCL technique has been chosen, slope limiters are used to preserve the TVD properties of scheme. $\mathbf{U}$ is approximated by the construction of linear air interpolation at the interface Γ_{ij}. This technique does not assure the monotonicity of the scheme, to overcome this difficulty, limitation technique must be used, so it must to call for MinMod limiter [11]:

$$U_{ij}^{l} = U_i + \frac{1}{2}\nabla U_i.\overline{G_iG_j}, \quad U_{ij}^{r} = U_j + \frac{1}{2}\nabla U_j.\overline{G_iG_j}, \tag{11}$$

where $G_i(x_i,y_i)$ and $G_j(x_j,y_j)$ are respectively the barycenter of cells T_i and T_j. $\left(\frac{\partial U_i}{\partial x}, \frac{\partial U_j}{\partial x}\right)$ is evaluated as the minimum points of the following quadratic function [11]:

$$\theta_i(X, Y) = \sum_{j\in m(i)} \left| U_i + (x_j - x_i)X + (y_j - y_i)Y - U_j \right|^2, \tag{12}$$

where $m(i)$ is the set of neighborhood triangles with the triangle T_i:

$$\begin{cases} \dfrac{\partial^{\lim} U_i}{\partial x} = \dfrac{1}{2}\left(\begin{array}{l}\min_{j\in m(i)}\operatorname{sgn}\left(\dfrac{\partial U_j}{\partial x}\right)+ \\ +\max_{j\in m(i)}\operatorname{sgn}\left(\dfrac{\partial U_j}{\partial x}\right)\end{array}\right)\min_{j\in m(i)}\left|\dfrac{\partial U_j}{\partial x}\right|, \\ \dfrac{\partial^{\lim} U_i}{\partial y} = \dfrac{1}{2}\left(\begin{array}{l}\min_{j\in m(i)}\operatorname{sgn}(\dfrac{\partial U_j}{\partial y})+ \\ +\max_{j\in m(i)}\operatorname{sgn}\left(\dfrac{\partial U_j}{\partial y}\right)\end{array}\right)\min_{j\in m(i)}\left|\dfrac{\partial U_j}{\partial y}\right|. \end{cases} \tag{13}$$

These values are used in the relation to value U_{ij}^{l} and U_{ij}^{r}, the numeric flux is calculated then by the Roe's scheme while using $\tilde{\mathscr{A}}\left(U_{ij}^{l}, U_{ij}^{r}\right)$.

3.3. Modification of the Roe scheme to handle dry regions

The Roe average is not defined when the left and right water levels of the element are equal to zero. Some modifications have then to be made in order to define the numerical flux. Here the following flux modifications are used:

– If the left and right water levels of the element are equal to zero, then:

$$\Phi\left(U_i, U_j\right) = 0; \tag{14}$$

– If the left water level of the element is equal to zero, and the right water level of the element is not equal to zero, then:

$$\Phi\left(U_i, U_j, n_{ij}\right) = \frac{1}{2}\left(\mathscr{F}\left(U_j, n_{ij}\right)\right) - \frac{1}{2}\left|\tilde{\mathscr{A}}\left(U_j, n_{ij}\right)\right|\left(U_j\right) \tag{15}$$

A formula similar to Eq. (15) is taken, when $h_i \neq 0$ and $h_j = 0$. These alterations allow calculations to go ahead to final iterations. However, an unphysical stationary jump can appears at the dam location, as the Roe scheme, even modified to handle dry regions, does not ensure the entropy condition, see Figs 1 and 2. The solution to this problem can be achieved by increasing the numerical dissipation where the numerical viscosity is low (see for instance [15]). Another approach is [16], which is considered here consists in introducing a rarefaction wave wherever the Roe scheme constructs invalid shocks. A correction is required, if the left and right sonic eigenvalues of same type have different signs, while representing a rarefaction:

$$\lambda_i<0<\lambda_j. \tag{16}$$

This situation may correspond to a nonphysical shock. To overcome the problem, the eigenvalues are modified. Depending on the simplification chosen, one of the following modifications on the average eigenvalue are required:

$$\lambda^* = \lambda_j\frac{\tilde{\lambda} - \lambda_i}{\lambda_j - \lambda_i}, \tag{17}$$

where $\tilde{\lambda}$ is the average eigenvalue are evaluated by considering the state variables mean of h, u and v. This equation is used if Eq. (10) is manipulated,

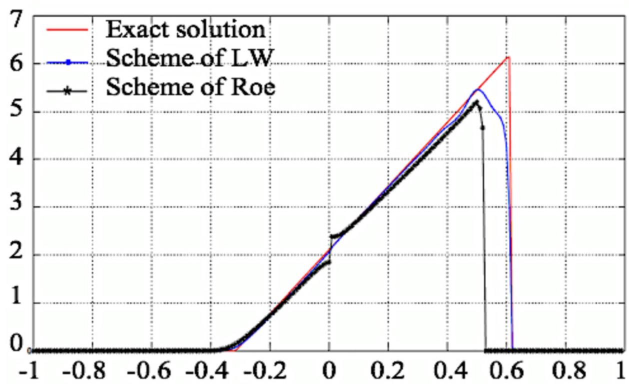

Fig. 1. 1D cross-section on u along the x-axis at time $t = 0.15$ sec

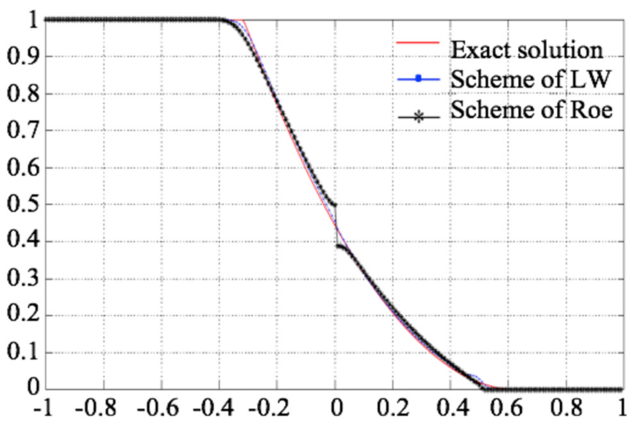

Fig. 2. 1D cross-section on h along the x-axis at time $t = 0.15$ sec

$$\lambda^{\star} = \lambda_i \frac{\lambda_i - \tilde{\lambda}}{\lambda_j - \lambda_i}. \quad (18)$$

3.4. Time integration

Since the model is applied to transient flows and flood waves and in order to obtain formally second order accuracy, the time integration is performed by means of a second order accurate and hardly dissipative explicit Runge-Kutta method. As with all explicit time stepping methods the theoretical maximum stable time step is specified according to the Courant-Friedrichs-Lewy (CFL) condition,

$$\Delta t = Cr\mathrm{Min}_{\Gamma_{ij}} \left[\frac{|T_i| + |T_j|}{2|\Gamma_{ij}|\mathrm{Max}\left|\lambda_{ij}^{p}\right|} \right]. \quad (19)$$

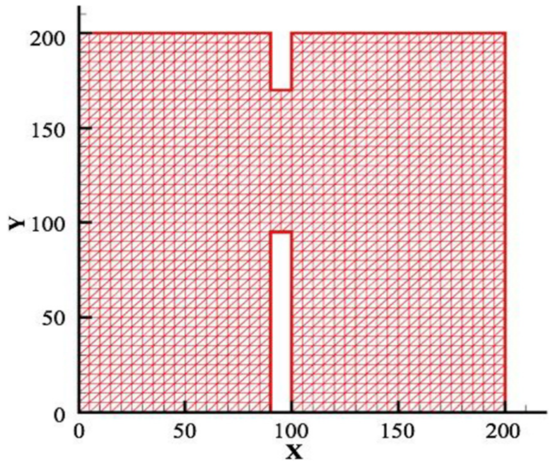

Fig. 3. Geometry and form of the study domain (triangular mesh of the domain)

4. NUMERICAL RESULTS

4.1. Partial dam break

The test case presents tow-dimensional dam break. The objective here is to verify the capacity of the model to reproduce the two-dimensional propagation of floods in the presence of a discontinuous front of the water height and the velocity on a dry flat bottom. The torrential flow due to partial and asymmetric dam break are considered [14].

This problem, which was proposed by [13] is widely used by many researchers to validate their dam break models. The particular interest is that its solution is characterized by:

– A shock wave which propagates downstream by abruptly increasing the water height and is modified by a reflection wave (when it collides with the wall);
– A rarefaction (depression) wave, which moves upstream by decreasing the water height, often described as a rarefaction shock.

The study area is a 200 m wide basin, 200 m long and has flat bottom, without friction. The water is retained in the left part of the basin. It is assumed that at $t = 0$ sec, suddenly the reservoir of the dam is in partial rupture and is non-symmetrical along a length of 75 m. The thickness of the dam is 10 m on the flow direction. Figure 3 gives a geometric description of this problem. The domain studied was discretized in 1,656 nodes and 3,100 triangles (Fig. 3) whose sizes are regularly fixed at 5 m. It should be noted that there is no analytical solution to this two-dimensional problem. A ratio of $h_2/h_1 = 0$ is initially fixed with $h_1 = 10$ m the water height in the reservoir and $h_2 \approx 0$ exactly, the water height downstream of the dam is fixed at $h_2 \approx 10^{-8}$ m for the finite element method and at $h_2 \approx 10^{-5}$ m (means that the bottom is almost dry, h is close to zero) for the finite volume method. The water in the basin is assumed to be at rest in the initial state.

To $t = 0$, the dam breaks and a wave of rise appears in the water level that propagates in the domain. The solution is calculated by the two schemes. Figures 4, 5 and 6 show the propagation of the flood wave along the opening of the dam at times of 1–5 s, a remarkable similarity is noted between

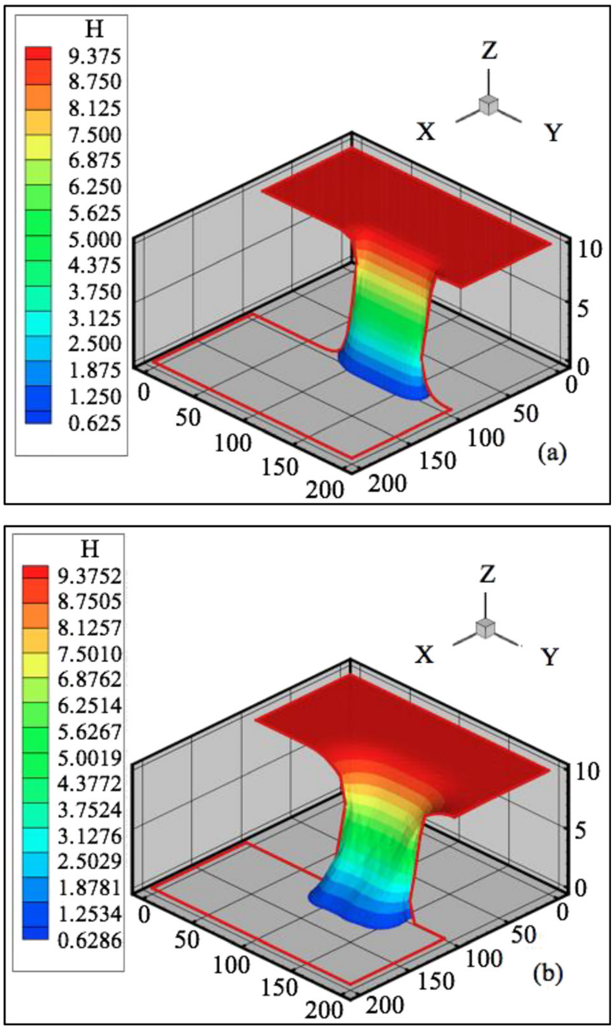

Fig. 4. Depth contour, a) Taylor–Galerkin scheme; b) scheme of modified Roe at $t = 3$s

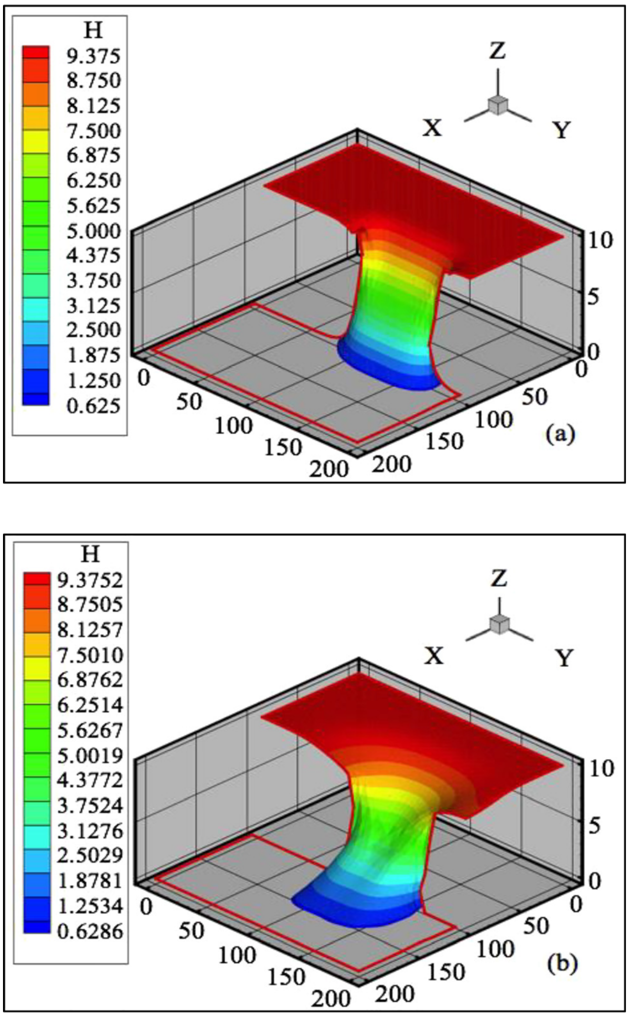

Fig. 5. Depth contour, a) Taylor–Galerkin scheme; b) Scheme of modified Roe at $t = 4$s

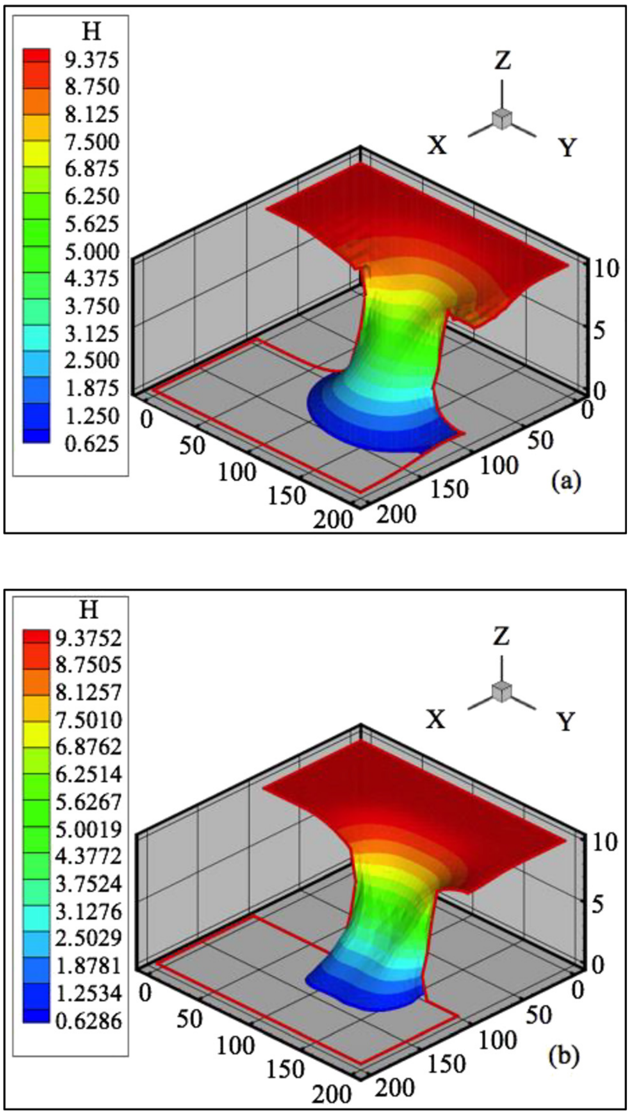

Fig. 6. Depth contour, a) Taylor–Galerkin scheme; b) Scheme of modified Roe at $t = 5$s

the two schemes. In order to better show the quality of the two schemes to reproduce the solution of the rupture of the dam, a cut is made along the dam at $y = 135$ m see Fig. 7. There is a good agreement between the two methods, with a slight diffusion given by the finite element scheme. Despite the similarity of the results of the two schemes, it is noted that the Taylor–Galerkin (TG) finite element scheme generates slight oscillation at the corners of the dam opening, even adding some numerical diffusion. This can be justified by the use of second-order centered schema. It is also estimated that the finite volume scheme is more accurate, less diffusive but more consuming in CPU time. However in finite element with this scheme it is possible to reach dry bed with $h = 10^{-8}$ m, but in modified Roe finite volume method, the dry bed cannot exceed $h = 10^{-5}$ m. This is justified by the use the diffusion term, with a parameter which is generally difficult to adjust.

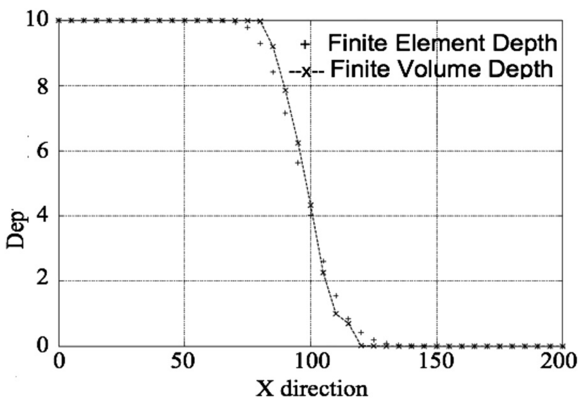

Fig. 7. Linear depth cut at $y = 135$ m, during $t = 1$ s

5. CONCLUSION

The study of this paper processes the shallow-water problem governed by Saint-Venant equations in conservatives variables, known for their hyperbolic characters. The numeric resolution is done by the method of the finite volumes coupled to the scheme of modified Roe. The dam break problem was simulated and compared on dry bed with a second order centered scheme written in finite element method. Similar results and good agreement are found between the two approaches for the dry bottom test, as conclusion, in two-dimensional problem, the two methods give comparable results, however, the Taylor Galerkin in finite element scheme is more diffusive and the oscillations persist in the rupture of the dam. This is due to the propagation of oscillations in infinity of direction of flow.

REFERENCES

[1] F. Boushaba, A. Grari, M. Chourak, Y. Regad, and B. Elkihel, "Numerical simulation of the flood risk of the deviation hydraulic structure at Saidia (North-East Morocco)," in *Proceedings of the 2nd International Conference on Electronic Engineering and Renewable Energy Systems*, Saidia, Morocco, April 13–15, 2020, pp. 659–665.

[2] F. Boushaba, A. Grari, M. Chourak, Y. Regad, and B. Elkihel, "Numerical simulation of the sediment transport of the hydraulic diversion structure in Saidia (North-East of Morocco)," in *Proceedings of the 2nd International Conference on Electronic Engineering and Renewable Energy Systems*, Saidia, Morocco, April 13–15, 2020, pp. 667–673.

[3] F. Boushaba, E. Chaabelasri, N. Salhi, I. Elmahi, F. Benkhaldoun, and A. G. L. Borthwick, "Comparative study of finite element and finite volume for problems of transcritical free surface flows on unstructured meshes," *Int. J. Comput. Methods*, vol. 05, no. 3, pp. 413–431, 2008.

[4] D. Marcsa and M. Kuczmann, "Performance study of domain decomposition methods for 2D parallel finite element analysis," *Pollack Period.*, vol. 8, no. 3, pp. 47–58, 2013.

[5] Y. Regad, B. Elkihel, F. Boushaba, and M. Chourak "Numerical study of the smoke plume of the Jerada thermal power plant Morocco," *Pollack Period.*, vol. 14, no. 2, pp. 119–130, 2019.

[6] J. M. Hervouet, "Telemac modeling system: an overview," *Hydrological Process*, vol. 14, no. 13, pp. 2209–2210, 2000.

[7] O. Delestre, F. Darboux, F. James, C. Lucas, C. Laguerre, and S. Cordier, "Full SWOF: A Free Software Package for the Simulation of Shallow Water Flows", Research Report, Hal-00932234. Institut National de la Recherche Agronomique, 2014.

[8] F. Alcrudo, and P. Garcia-Navarro, "A high- resolution Godunov type scheme in finite volumes for the 2D shallow-water equations," *Int. J. Numer. Methods Fluids*, vol. 16, no. 6, pp. 489–505, 1993.

[9] M. E. Vazquez-Cendon, "Improved treatment of source terms in upwind schemes for the shallow water equations in channels with irregular geometry," *J. Comput. Phys.*, vol. 148, no. 2, pp. 497–526, 1999.

[10] J. G. Zhou, D. M. Causon, C. G. Mingham, and D. M. Ingram, "The surface gradient method for the treatment of source terms in the shallow water equations," *J. Comput. Phys.*, vol. 168, pp. 1–25, 2001.

[11] F. Benkhaldoun, I. Elmahi, and M. Seaïd, "A new finite volume method for flux-gradient and source-term balancing in shallow water equations," *Comput. Methods Appl. Mech. Eng.*, vol. 199, nos 49–52, pp. 3324–3335, 2010.

[12] P. L. Roe, "Approximate Riemann solvers, parameter vectors, and difference schemes," *J. Comput. Phys.*, vol. 43, no. 2, pp. 357–372, 1981.

[13] M. Seaïd, "Non-oscillatory relaxation methods for the shallow water equations in one and two space dimensions," *Int. J. Numer. Methods Fluids*, vol. 46, no. 5, pp. 457–484, 2004.

[14] Y. Lakhlif, S. Daoudi, and F. Boushaba, "Dam-break computations by a dynamical adaptive finite volume method," *J. Appl. Fluid Mech.*, vol. 11, no. 6, pp. 1543–1556, 2018.

[15] E. Godlewski and P. A. Raviart, *Hyperbolic Systems of Conservation Laws*. Ellipses, 1991.

[16] A. Harten and J. M. Hyman, "Self-adjusting grid methods for one dimensional hyperbolic conservation laws," *J. Comput. Phys.*, vol. 50, no. 2, pp. 235–269, 1983.